Tumour Response to Cabozantinib in a Transgenic Mouse Model of Neuroblastoma Assessed by Multiparametric MRI

Gilberto S. Almeida[1], Philippa King[2], Yann Jamin[1], Albert Hallsworth[2], Hannah Webber[2], Sergey Popov[3], Louis Chesler[2], and Simon P. Robinson[1]

[1]*Radiotherapy and Imaging, The Institute of Cancer Research, Sutton, Surrey, United Kingdom,* [2]*Clinical Studies, The Institute of Cancer Research, Sutton, Surrey, United Kingdom,* [3]*Molecular Pathology, The Institute of Cancer Research, Sutton, Surrey, United Kingdom*

Introduction: Neuroblastoma (NB) is the most common extra-cranial solid tumour in childhood, accounting for ~15% of paediatric cancer-related deaths. The proto-oncogene *MYCN* is amplified in 25% of NB, and is associated with enhanced angiogenesis and poor survival (1). Vascular endothelial growth factor (VEGF) is the most potent angiogenic growth factor and, with the hepatocyte growth factor (HGF)/c-MET signalling pathway, is implicated in the progression of human NB (2). Cabozantinib (CBZ) is a small-molecule kinase inhibitor with potent activity against VEGFR2 and MET (3), and is currently in clinical trials against NB. Using multiparametric MRI, and pathological correlates, this study evaluated the efficacy of CBZ in the TH-*MYCN* GEM model of high-risk NB, previously shown to faithfully recapitulate the radiological and hypervascular characteristics of childhood NB (4,5).

Methods: TH-*MYCN* mice with spontaneous abdominal tumours were imaged prior to and 48 hours after daily treatment with either vehicle (n=6) or 30mg/kg CBZ (n=10). Images were acquired on a 7T horizontal MicroImaging system using a 3cm birdcage coil, using 128 phase encoding steps over a 3x3cm FOV. Abdominal T_2-weighted images were acquired from 20 contiguous 1mm thick coronal slices using a RARE sequence (TE=36ms,TR=4.5sec), used to localise and quantify tumour volume through segmentation of ROIs drawn on each tumour-bearing slice. Native T_1 was quantified from a single transverse 1mm thick slice through the tumour centre using an IR-trueFISP sequence (TE=1.2ms, TR=2.4ms). Tumour R_2* was quantified from three 1mm thick transverse sections through each tumour using a multigradient echo (MGE) sequence (TE=6-27ms, 8 echoes, TR=200ms). Diffusion-weighted (DW) images were acquired using an EPI sequence acquired from the same three 1mm thick transverse sections (TE=32ms, TR=1500ms, 5 b-values 200-1000s/mm^2). Parametric maps of native T_1, R_2* and ADC were generated by fitting the IR-trueFISP, MGE and DW MRI data voxelwise using in-house software. Tumour necrosis and microvessel density (MVD) were scored on tumour sections stained with haematoxylin and eosin (H&E), or immunohistochemically processed for the vascular endothelial marker CD34. Statistical significance was identified using Student's 2-tailed t-test with a 5% level of significance.

Results: Pre-treatment values of tumour native T_1 and R_2* were in good agreement with those previously reported in the TH-*MYCN* model (5,6). Treatment with CBZ induced highly significant tumour growth arrest compared to control. This was associated with significant decreases in both T_1 and R_2* (Figs. 1&2, Table 1), but no significant difference in ADC. Histopathological analysis revealed a significant increase in necrosis, and significant decrease in MVD, in CBZ-treated tumours compared to control (Fig. 3).

Discussion & Conclusion: This study demonstrates that CBZ is efficacious against the TH-*MYCN* GEM model of NB, and establishes native T_1 and R_2* as early non-invasive biomarkers of response to CBZ in NB. The data also reinforces native T_1 as a biomarker of response to anti-vascular therapy, due to its sensitivity to therapy-induced damage to erythrocytes and/or cell death-mediated increase in macromolecules into the extracellular space (5,7). Relatively fast R_2* rates in NBL arising in the TH-*MYCN* model are strongly associated with vascular instability, characterised by numerous regions of aggregated deoxygenated paramagnetic erythrocytes ("blood lakes", Fig. 3) (6), and treatment-induced thrombosis with the pan-VEGFR inhibitor cediranib increased tumour R_2* (5). Interestingly, the CBZ-induced decrease in tumour R_2* seen herein is clearly associated with vascular disruption, hence precluding the extravasation of deoxygenated red blood cells.

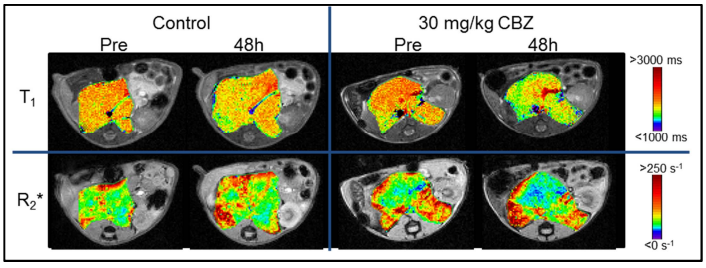

Fig. 1: *Parametric T_1 and R_2* maps acquired from control and CBZ-treated TH-MYCN transgenic mice.*

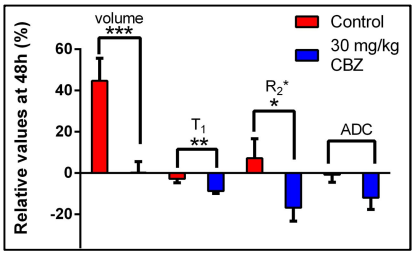

Fig. 2: *Relative values 48 hours post-treatment.*

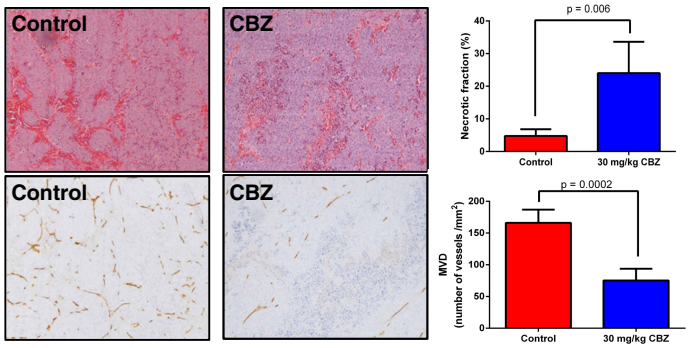

Fig. 3: *H&E and CD34 stained sections from control and CBZ-treated tumours, and quantitation of necrosis and MVD.*

Table 1	Control (n=6)		30mg/kg CBZ (n=10)	
	Pre	48h	Pre	48h
Volume (mm^3)	930 ± 430	1304 ± 544*	781±68	775±76
T_1 (ms)	1805 ± 30	1753 ± 22	1812 ± 17	1652 ± 18***
R_2* (s^{-1})	104 ± 16	106 ± 11	123 ± 8	104 ± 9*
ADC (x10^6 mm^2 s^{-1})	682 ± 46	676 ± 48	687 ± 45	588 ± 28

References: (1) Meitar *et al*, J Clin Oncol, 1996. (2) Choudhury *et al*, J Oncol, 2011. (3) Yakes *et al*, Mol Cancer Ther, 2011. (4) Weiss *et al*, EMBO J, 1997. (5) Jamin *et al*, Radiology, 2013. (6) Jamin *et al*, PLoS ONE, 2014. (7) McSheehy *et al*, Clin Cancer Res, 2010.

Acknowledgements: Supported by Cancer Research UK (grant #C1060/A10334), EPSRC (grant #EP/H046526/1), The Wellcome Trust (grant #091763Z/10/Z) and Children with Cancer UK.